Understanding the Atomic-Scale Origins of Radiation Damage in Semiconductor Devices through Electron Paramagnetic Resonance Measurements

Jason T. Ryan, Ph.D.
Project Leader – Magnetic Resonance Spectroscopy
Alternative Computing Group
Nanoscale Device Characterization Division
Jason.Ryan@nist.gov

NIST National Institute of Standards and Technology
U.S. Department of Commerce

PML
PHYSICAL MEASUREMENT LABORATORY

Motivation

- Explosive growth of semiconductor industry changing the very fabric of society.

3 Tech Growth Strategies for 2021 to Navigate Uncertainty, M. Kopelman (2021), www.apiro.com

Technology: Growth and Impact, MM. Crapis, (2019). Zeutek.com

How?

- Lots of reasons…
- Key Fuel - faster and cheaper fundamental building blocks (transistors).

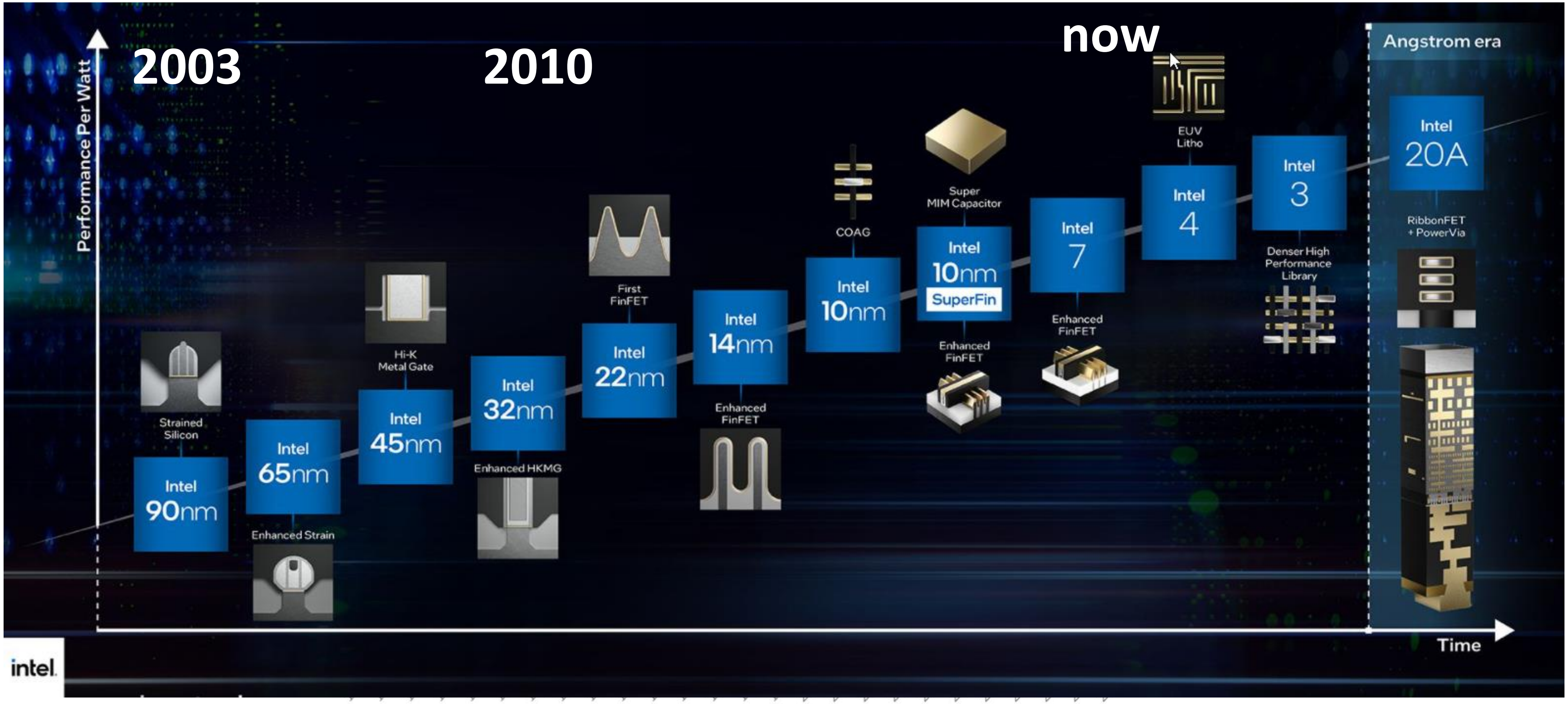

Data source: Wikipedia (wikipedia.org/wiki/Transistor_count) Year in which the microchip was first introduced

*technology node has become a marketing tool rather than a real physical feature description

Transistor operation for logic (MOSFET)

- **Metal-oxide-silicon/semiconductor field-effect-transistor.**
- Basic operation all comes down to 1's and 0's (on and off).

What makes a "better" transistor?

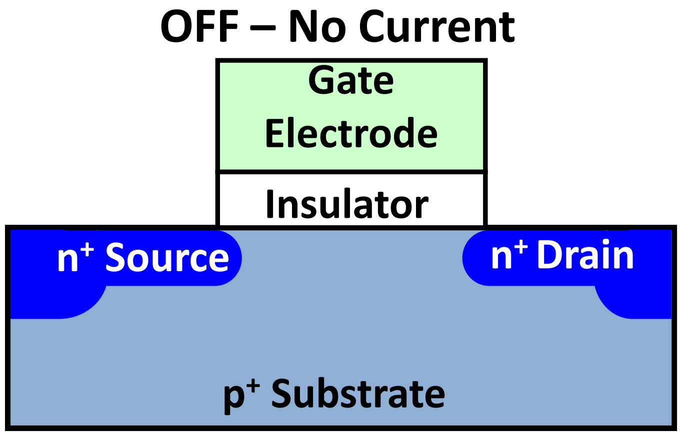

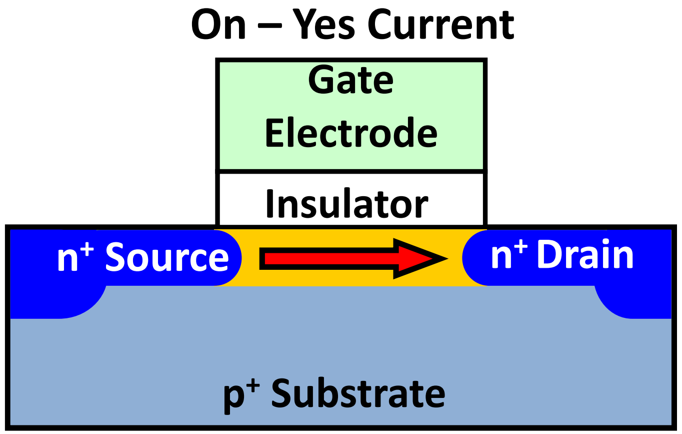

CMOS: Complimentary metal-oxide-semiconductor – mix of MOSFET "flavors" (nMOS & pMOS).

Why defects matter

Defects or “tra

Available or Forbidden Energy Levels

Quantum Mechanical Tunneling Defect

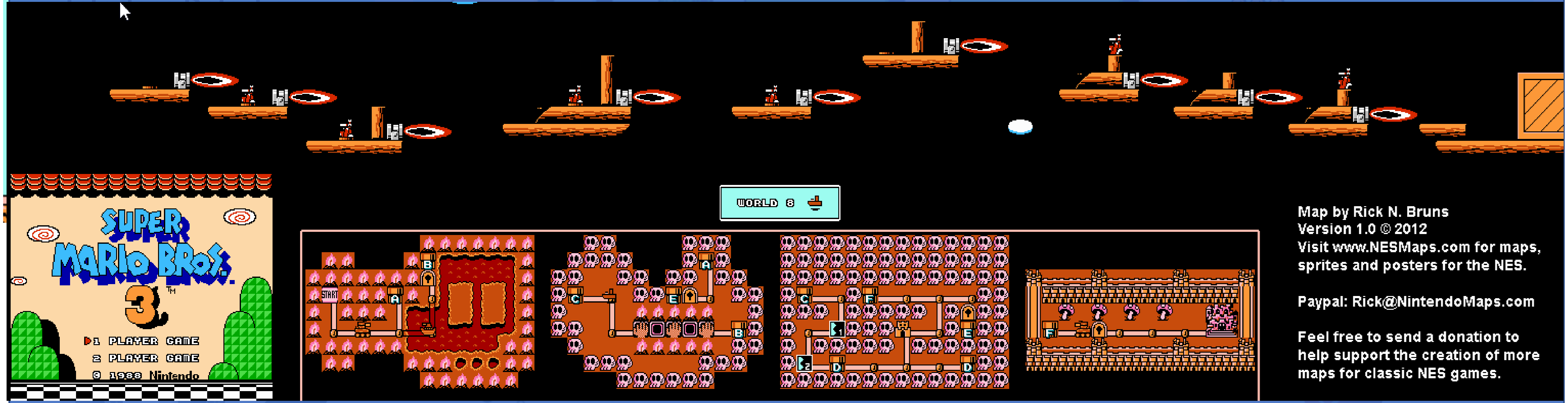

New device, technology, material, etc. (if you're lucky).
Ex. badly damaged due to radiation.
Only getting more complicated.
Practice makes perfect.

The Semiconductor Industry – Defect Problem

- Do bad things.
- Unavoidable.
- Increasingly Important.
  - Scaling (individual atoms matter).
  - Materials (more complicated species).
  - Design (more complicated interactions).

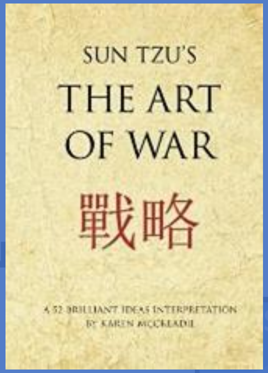

"So it is said that if you know your enemies and know yourself, you can win a hundred battles without a single loss."—Sun Tzu

Electron Paramagnetic Resonance; an Imperfect Analogy…

Photo Credit: gehealthcare.com

Photo Credit: medicaldevice-network.com

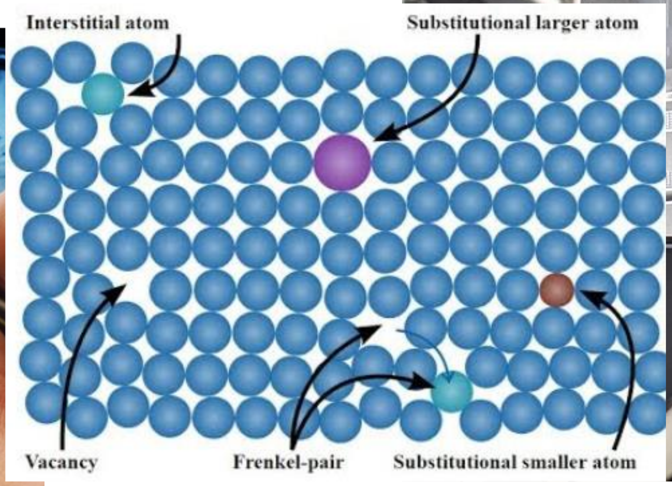

Photo Credit: youtube.com

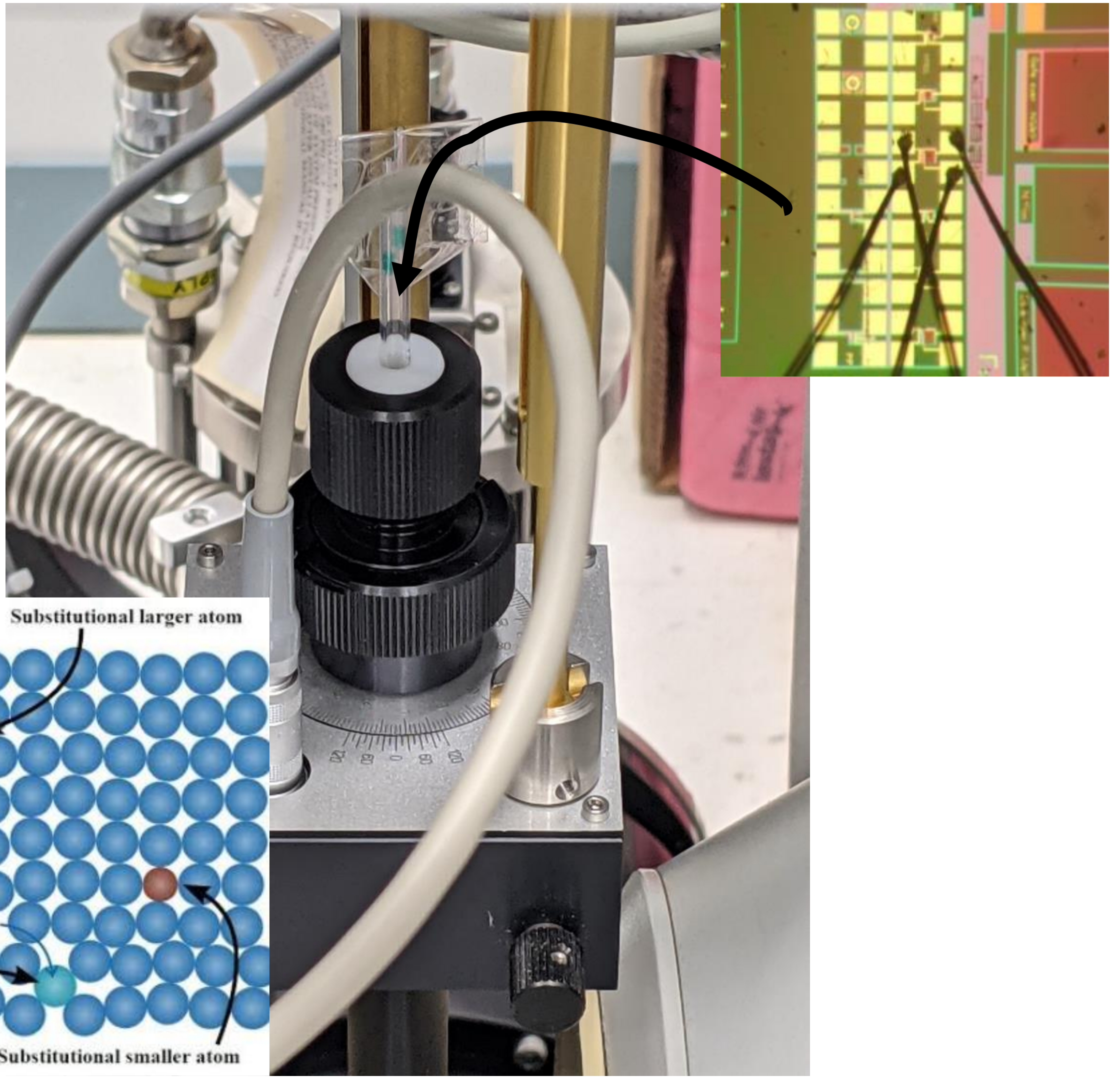

Experimental Modes…

- **Conventional Electron Paramagnetic/Spin Resonance**
  - Unrivaled access to atomic scale chemical and physical nature.
  - Large area/volume samples.
  - Great for “simple” material structures.

- **Electrically Detected Magnetic Resonance (EDMR)**
  - Detect EPR via resonance induced change in device current.
  - Fully processed nanoscale devices.
  - Same EPR information directly linked to device operation.
  - Many modes of operation (specialized information).

What information are we after?

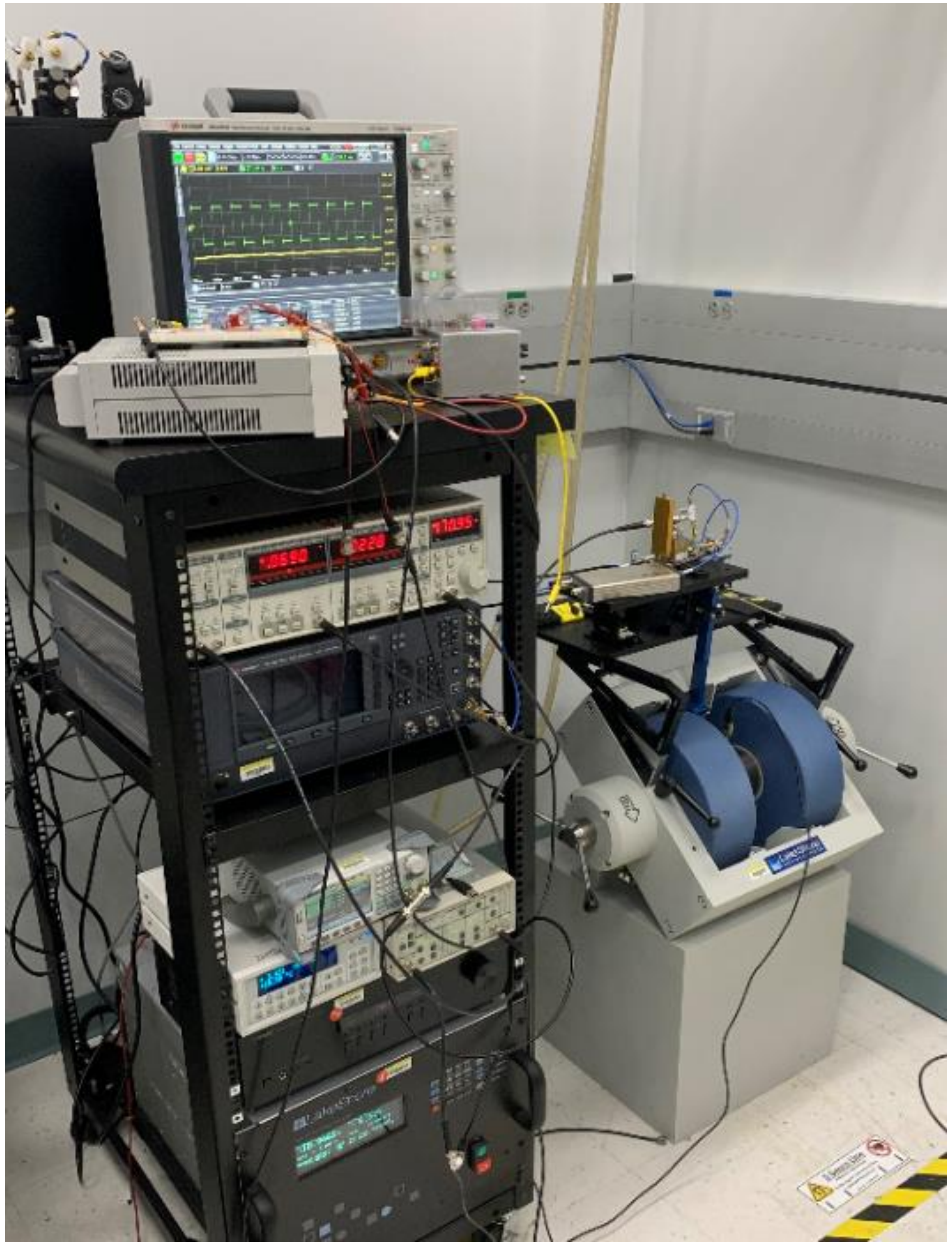

Example 1: Conventional EPR, Interface Defects Si/SiO_2

IEEE Transactions on Nuclear Science, Vol. NS-28, No. 6, December 1981

RADIATION-INDUCED TRIVALENT SILICON DEFECT BUILDUP AT THE $Si\text{-}SiO_2$ INTERFACE IN MOS STRUCTURES

P. M. Lenahan, K. L. Brower, and P. V. Dressendorfer
Sandia National Laboratories
Albuquerque, New Mexico 87185

W. C. Johnson
Department of Electrical Engineering and Computer Science
Princeton University
Princeton, New Jersey 08544

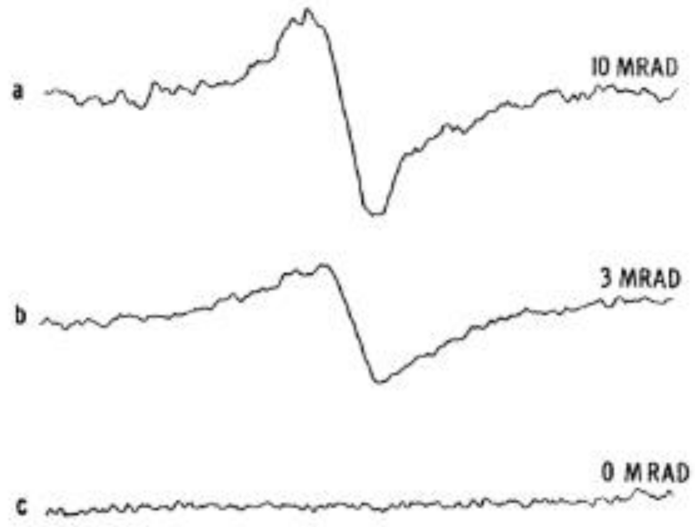

Figure 1. ESR spectra of three samples are illustrated. Non-saturating microwave power, cavity Q and sample size are essentially identical. Samples a, b, and c were exposed to respectively 10 Mrad, 3 Mrad, and 0 Mrad of Co^{60} gamma irradiation.

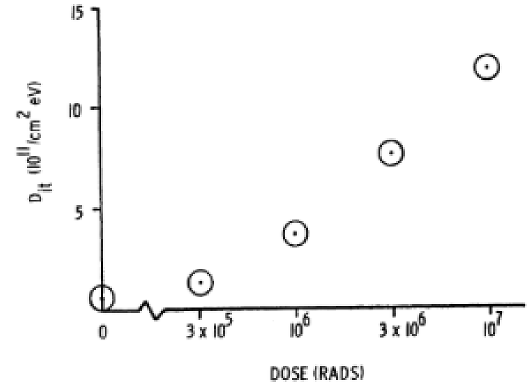

Figure 2. Average interface state density D_{it} in mid 0.5 eV of band gap vs. radiation fluence.

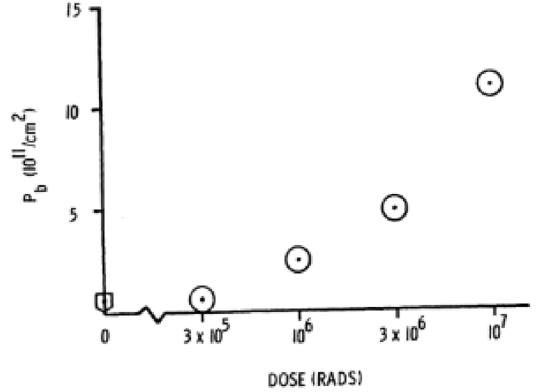

Figure 3. Density of trivalent silicon defects at the $Si\text{-}SiO_2$ interface measured with ESR. The arrow at zero fluence indicates that we were unable to observe the P_b resonance at this level of irradiation. We estimate that its concentration is less than 0.7 x $10^{11}/cm^2$.

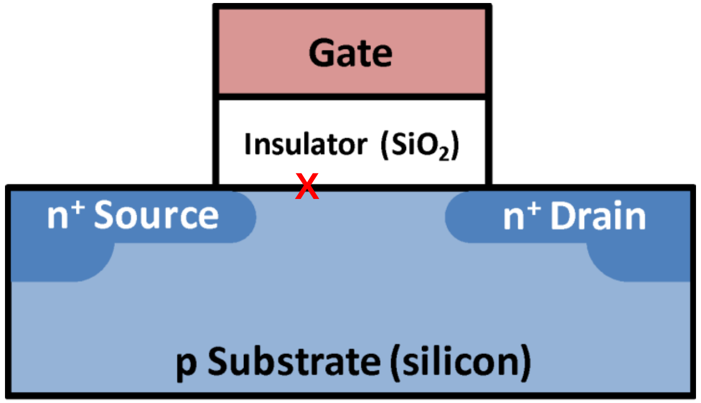

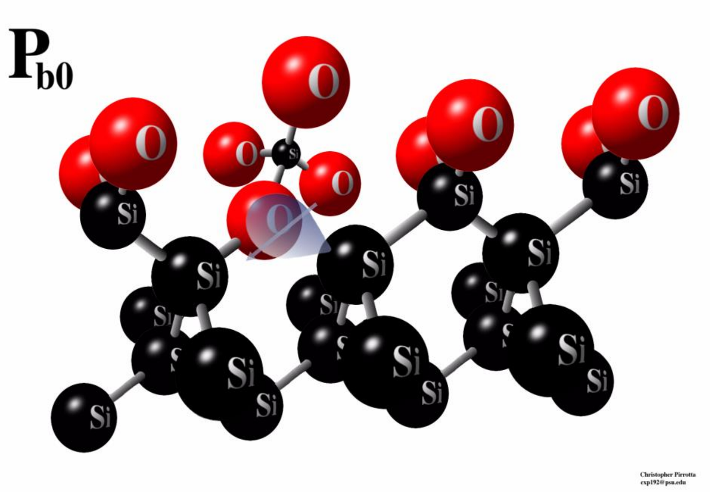

Example 2: Conventional EPR, oxide defects Si/SiO_2

Hole traps and trivalent silicon centers in metal/oxide/silicon devices

P. M. Lenahan and P. V. Dressendorfer
Sandia National Laboratories, Albuquerque, New Mexico 87185

(Received 21 November 1983; accepted for publication 14 December 1983)

3495 J. Appl. Phys. 55 (10), 15 May 1984 0021-8979/84/103495-05$02.40 3495

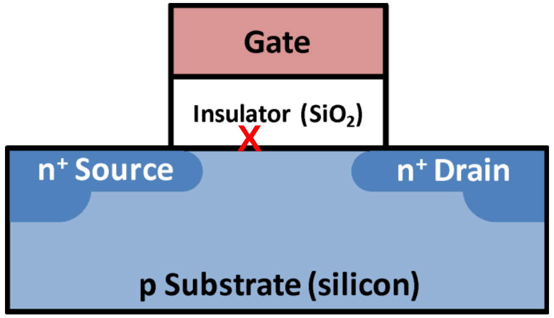

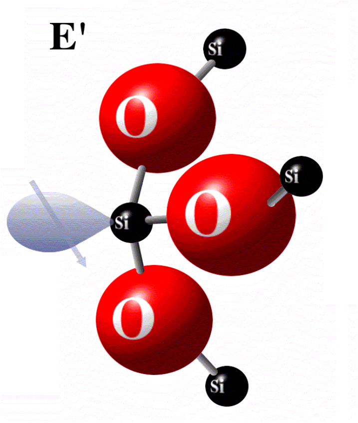

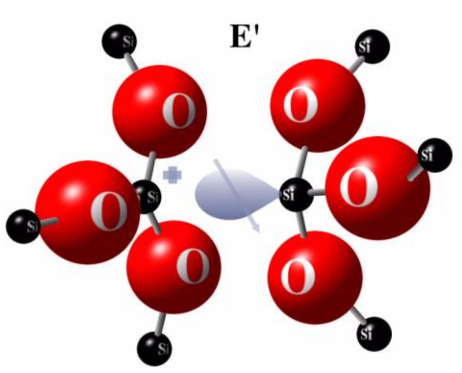

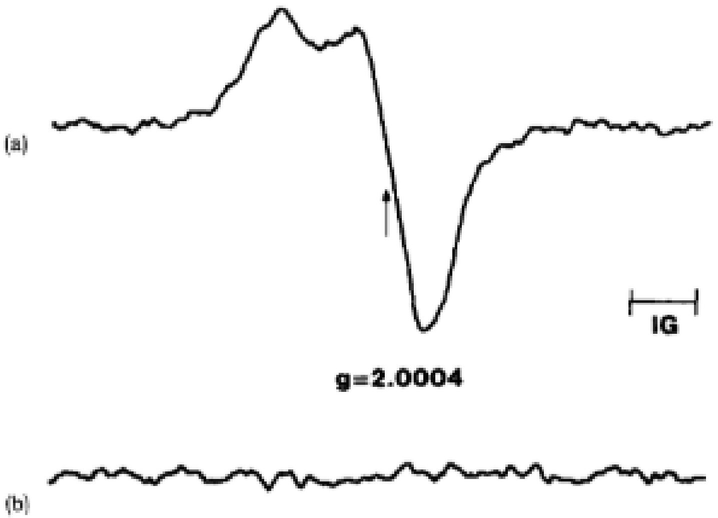

FIG. 3. ESR traces of identical samples (a) after exposure to 10 Mrad of Co^{60} γ-irradiation and (b) before exposure. The sample gates were positively biased to 20 V during irradiation. The E' center resonance is observed in (a).

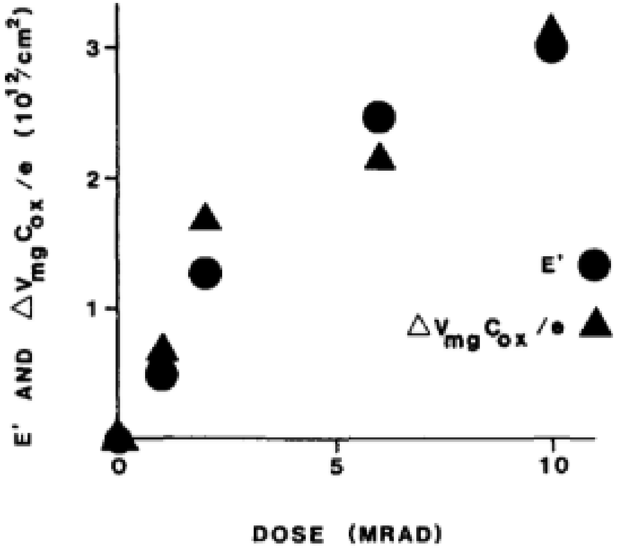

FIG. 4. Distributions of E' and $\Delta V_{mg} C_{ox}/e$ vs irradiation dose for MOS structures with oxides grown in dry oxygen and subjected to a nitrogen anneal.

Example 3: Conventional EPR, interface and oxide defects $Si/SiO_2/HfO_2$

2272 IEEE TRANSACTIONS ON NUCLEAR SCIENCE, VOL. 52, NO. 6, DECEMBER 2005

Identification of the Atomic Scale Defects Involved in Radiation Damage in HfO_2 Based MOS Devices

J. T. Ryan, *Student Member, IEEE*, P. M. Lenahan, *Member, IEEE*, A. Y. Kang, *Member, IEEE*, J. F. Conley, Jr., *Senior Member, IEEE*, G. Bersuker, *Member, IEEE*, and P. Lysaght

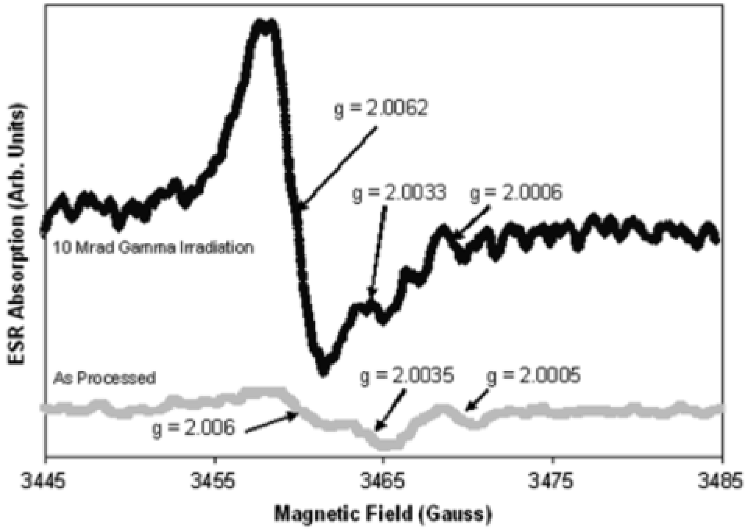

Fig. 1. Pre-irradiation (below) and post-irradiation (above) narrow scan ESR traces indicating the generation of large ($>10^{12}/cm^2$) densities of P_{b0} like Si/dielectric interface traps in the $HfCl_4$ precursor (sample set 1) HfO_2 dielectric film on SiO_2/silicon. (Weak signals are present in the pre-irradiation trace at $g = 2.006$, $g = 2.0035$, and $g = 2.0005$ which are respectively due to P_{b0} like interface traps, P_{b1} like interface traps and E' like oxygen deficient silicon near interface traps.)

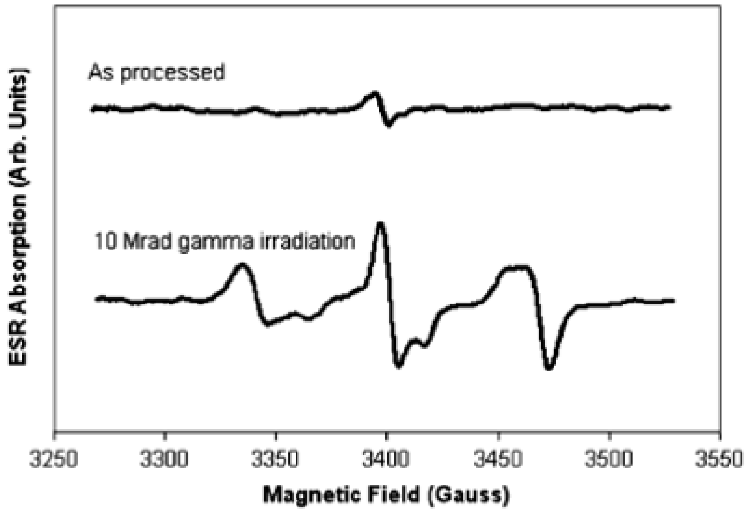

Fig. 2. Pre-irradiation (above) and post-irradiation (below) wide scan ESR traces indicating the generation of several defects in the $Hf(NO_3)_4$ precursor (sample set 2) HfO_2 dielectric film on H-terminated silicon. The two peaks on the left are (mostly) due to an O_2^- coupled to a hafnium ion (the central peak includes a small contribution from P_{b0} centers). The peak on the far right is likely due to an oxygen vacancy in the HfO_2. In these traces, the spectrometer settings have been set to optimize the O_2^- and oxygen vacancy spectra.

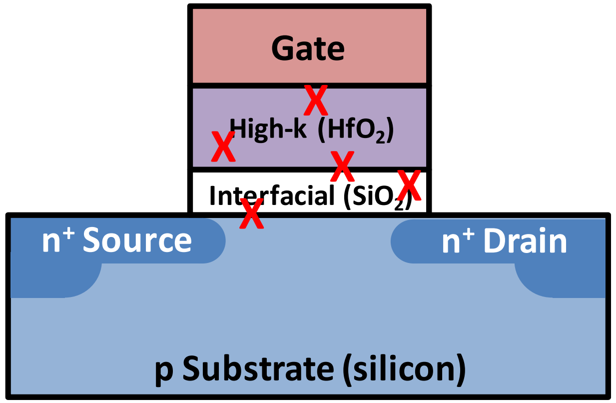

***much more complicated system due to "smeared" interfacial region and presence of hafnium.**

Example 4: EDMR, variety of modes and device structures

428 IEEE TRANSACTIONS ON NUCLEAR SCIENCE, VOL. 66, NO. 1, JANUARY 2019

A New Analytical Tool for the Study of Radiation Effects in 3-D Integrated Circuits: Near-Zero Field Magnetoresistance Spectroscopy

James P. Ashton, *Student Member, IEEE*, Stephen J. Moxim, *Student Member, IEEE*, Patrick M. Lenahan, *Fellow, IEEE*, Colin G. McKay, *Student Member, IEEE*, Ryan J. Waskiewicz, *Student Member, IEEE*, Kenneth J. Myers, *Student Member, IEEE*, Michael E. Flatté, *Member, IEEE*, Nicholas J. Harmon, and Chadwin D. Young, *Member, IEEE*

a-SiOC:H

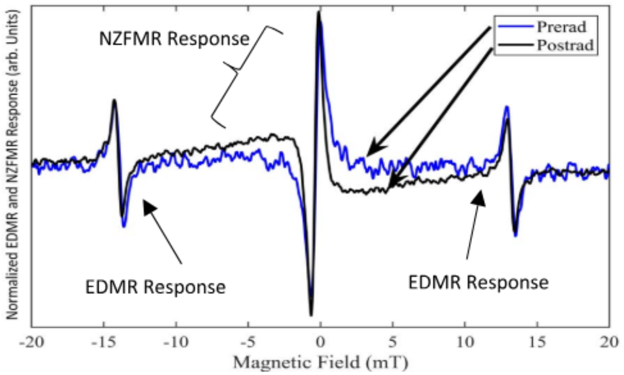

Fig. 16. Low field and frequency (360 MHz) EDMR and NZFMR response for a-SiOC:H dense samples for preirradiation (blue line) and postirradiation (black line) utilizing SDTAT. The modulation amplitude was 0.3 mT. The RF source output power used was approximately 40 mW.

Flowable oxide

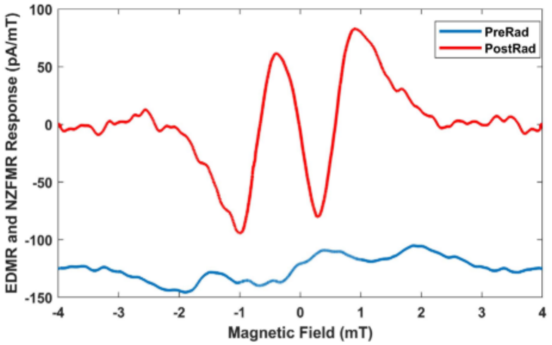

Fig. 14. Low field and frequency (72 MHz) EDMR and NZFMR response for SiO_2-based flowable oxides for preirradiation (bottom blue) and postirradiation (top red) utilizing SDTAT. The tunneling current was 2.2 μA. The modulation amplitude was 0.35 mT. The RF source output power used was approximately 20 mW. Note that the EDMR response is below the detection limit. Equivalent traces with RF turned off are identical. The spectra are offset from one another by −125 pA/mT.

Planar Si/SiO_2

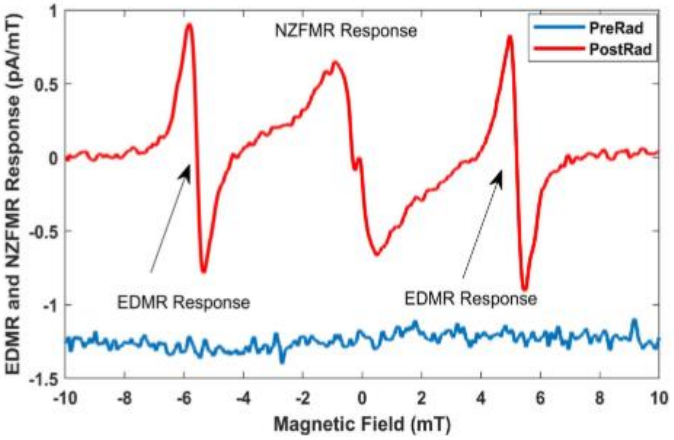

Fig. 8. Low field and frequency (151 MHz) EDMR and NZFMR response for planar Si/SiO_2 gated diodes for preirradiation (bottom blue) and postirradiation (top red) utilizing dc I–V. The forward bias used was 0.33 V. The modulation amplitude was 0.3 mT. The RF source output power used was approximately 1 W. The spectra are offset from one another by −1.25 pA/mT.

HKMG - SiGe

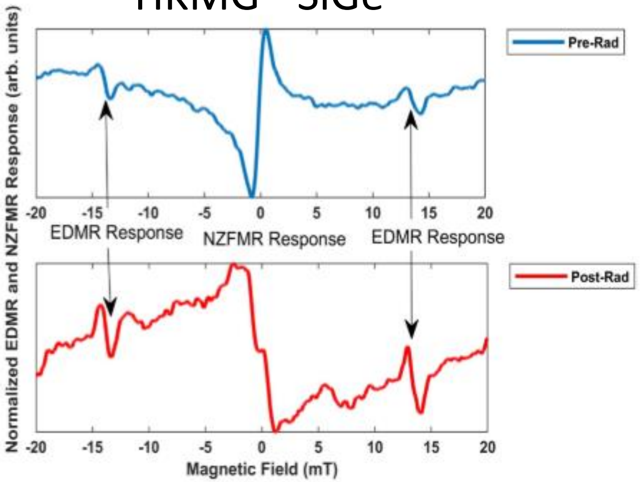

Fig. 10. Low field and frequency (365 MHz) EDMR and NZFMR response for lateral SiGe MOSFETs for preirradiation (top blue) and postirradiation (bottom red) utilizing SDCP. The charge-pumping frequency was 1 MHz and the pulse height used was 1.6 Vpp. The modulation amplitude was 1 mT. The RF source output power used was approximately 40 mW. The figures are normalized to illustrate differences in a line shape.

HKMG - FinFET

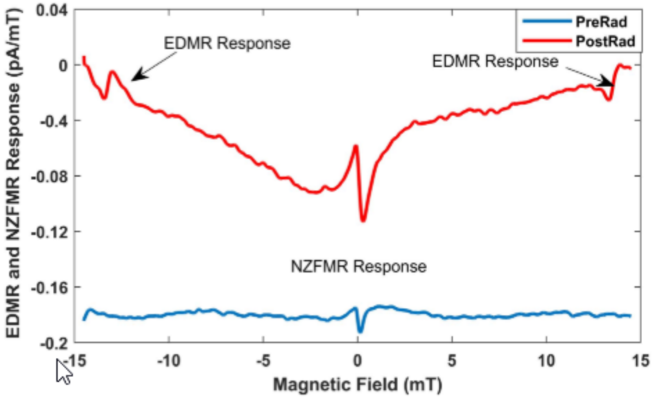

Fig. 12. Low field and frequency (375 MHz) EDMR and NZFMR response for Si FinFETs with a preirradiation (bottom blue) and postirradiation (top red) utilizing dc I–V. The forward bias used was −0.5 V. The modulation amplitude was 0.5 mT. The RF source output power used was approximately 40 mW. The spectra are offset from one another by −0.18 pA/mT.

Example 5: Resistive Memory Applications

Integral to many alternative computing schemes including neural networks and memory classes.

- Predictable behavior and adaptability require much broader physical understanding.
- Fundamental details regarding defect kinetics are still not resolved.
- Effects of traditional “reliability” problems not well understood in neural network applications.

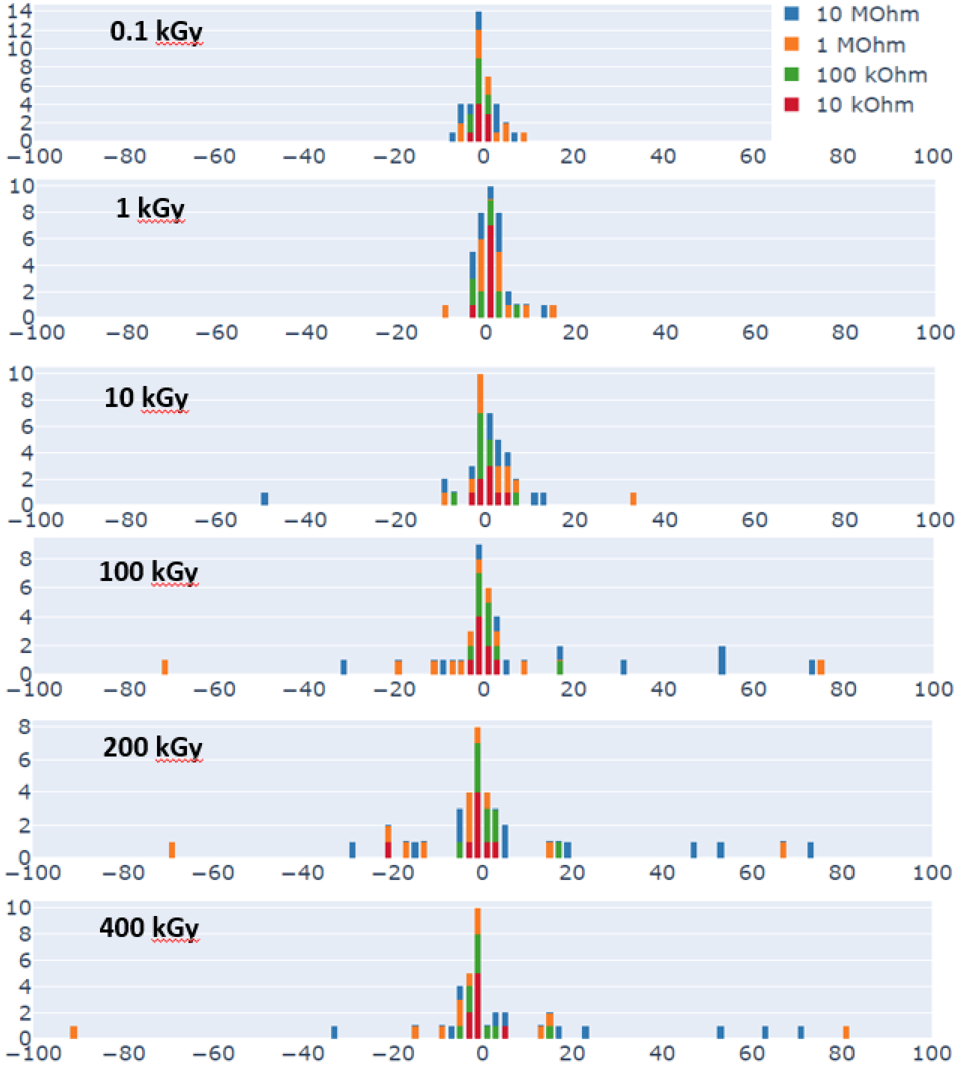

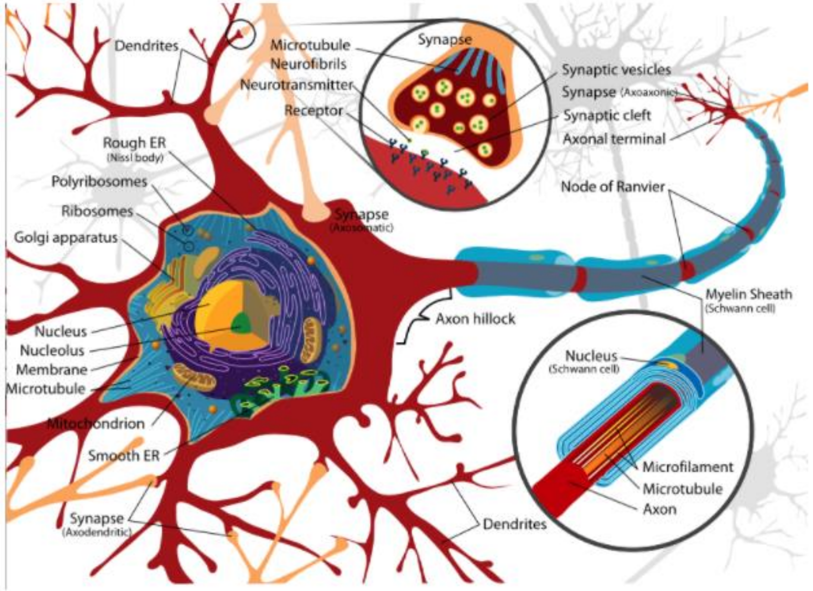

Fig. 1: Neuron cell diagram. Source: Wikimedia Commons.

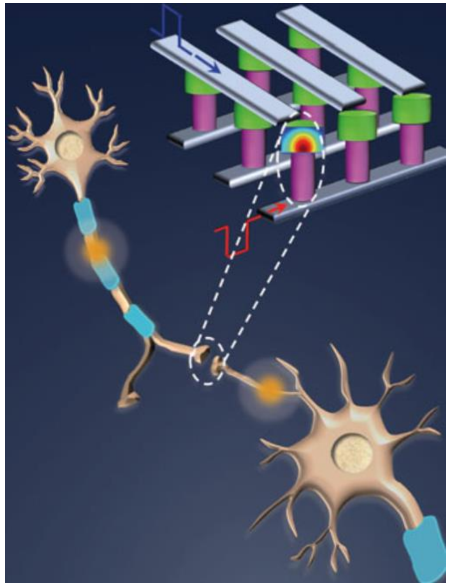

Photo Credit: nanowerk.com

Select Publications: M.A. Anders, et. al., *Appl. Phys. Lett, in prep, 2021.*, 1004, 573-580, 2020; M.A. Anders et. al., *J. Appl. Phys, 128 (24), 244501, 2020;* JP Ashton, et. al., *IEEE Intl. Reliab. Phys.*, 2019; M Anders, et. al., *APL*, 2019; D.J. McCrory, et. al., *Rev. Sci Inst.*, **90**, 014708, 2019; D.J. McCrory, et. al., *IEEE Trans. Nuc. Sci.*, 65 (5), 2018; G. Bersuker, et. al., *J. Comp. Elec.*, **16** (4), 2017.

Resources

- **Bruker ELEXSYS spectrometer.**
  - Conventional X-band ESR or EDMR.
  - Cryogen-free helium and nitrogen variable temp. (4 K - 1000 °C).
  - Programable goniometer.
  - In-situ UV irradiation.
- **1.5x homemade EDMR spectrometers.**
  - Multipurpose/reconfigurable.
  - Zero field through X band.
  - SDR, SDT, SDCP, BAE, etc…
- **Semiauto wafer prober w/ full IV, pulsed, and CV hardware.**
- **Manual wafer prober w/ full IV, pulsed, and CV hardware.**
  - Configurable to wafer-level EDMR system.
- **Staff**
  - Jason Ryan (PI) and Steve moxim (NRC PD).
  - Countless int./ext. collaborators.

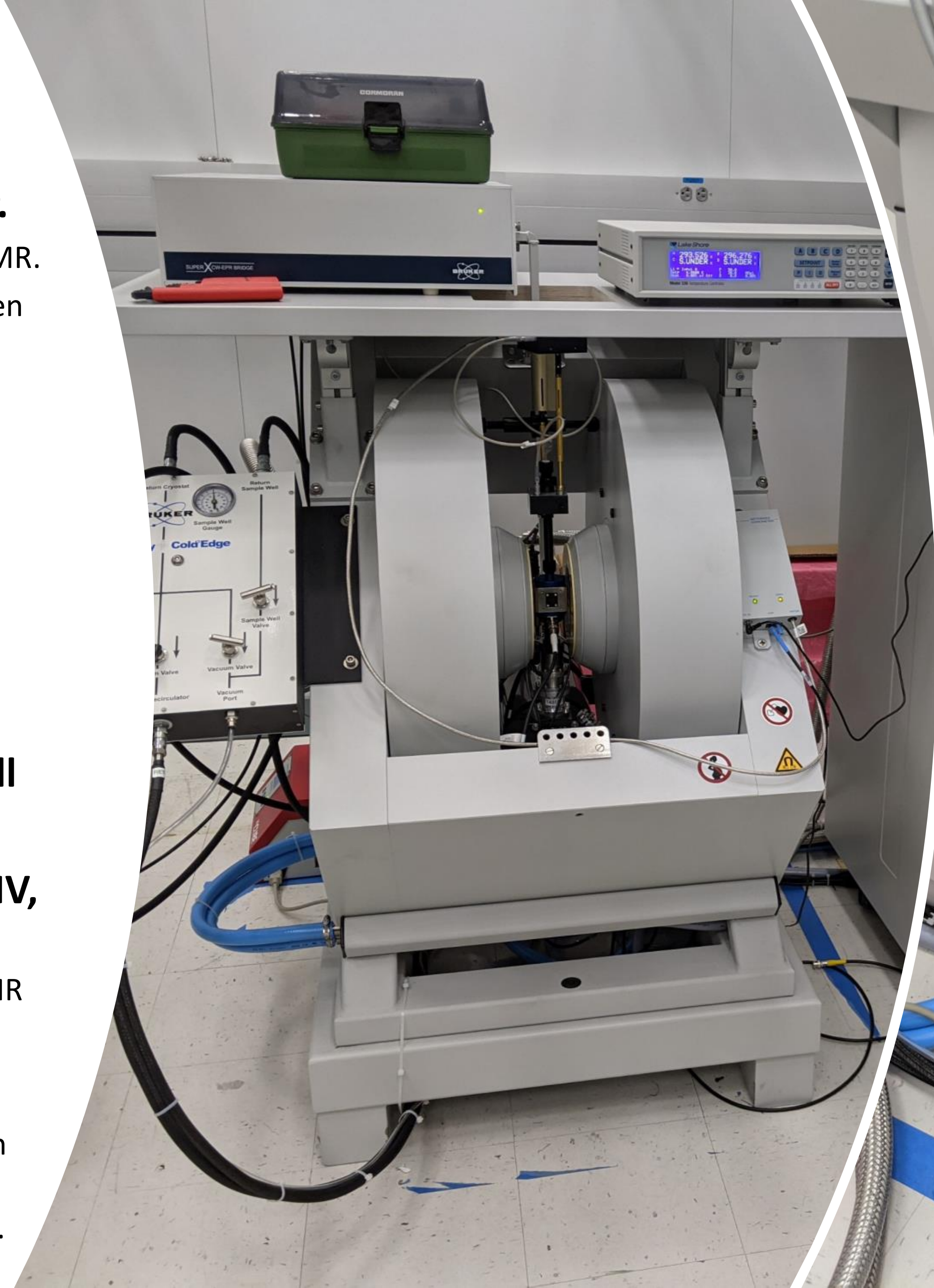

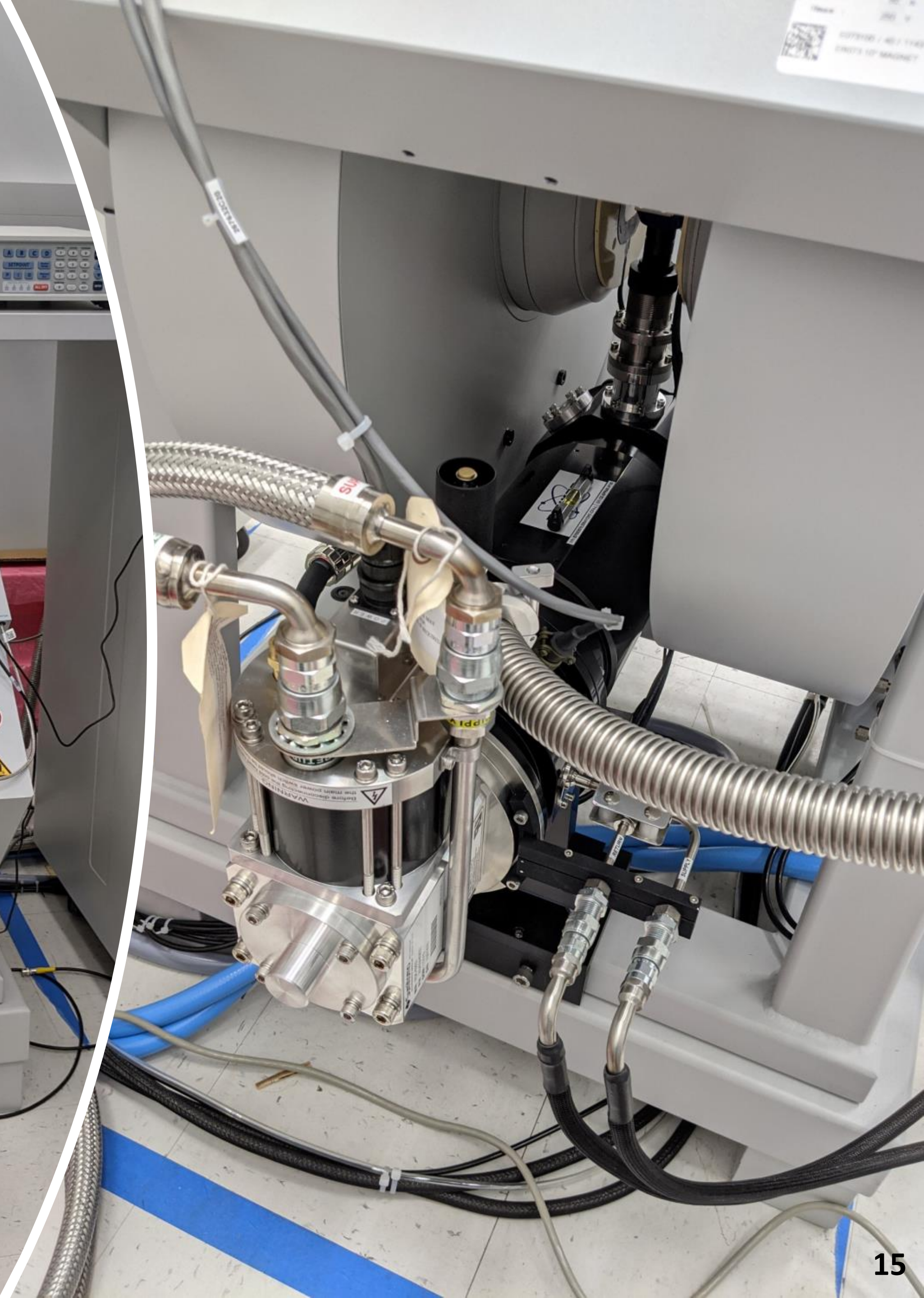

Summary

- **Explosive growth of semiconductor industry changing fabric of society.**
  - **fueled by "faster-cheaper-better" fundamental building blocks**
- **As technology advances defects become increasingly more important.**
  - **Individual atomic-scale defects matter (size).**
  - **Extremely complex materials systems.**
  - **Generated through normal use, including radiation exposure.**
- **Electron paramagnetic resonance a very powerful tool.**
  - **Understand chemical and physical nature.**
  - **Link back to actual device performance and operation.**
  - **Many examples of utilizing EPR to understand radiation damage at device/material level.**
- **Many example of utilizing EPR to understand radiation damage at device/material level.**
  - **Simple planar Si/SiO_2 MSOFETs through modern highly-complex 3D transistors.**

Example 5: EDMR, specialized per needs due to increased complexity…

228 IEEE TRANSACTIONS ON NUCLEAR SCIENCE, VOL. 67, NO. 1, JANUARY 2020

Observation of Radiation-Induced Leakage Current Defects in MOS Oxides With Multifrequency Electrically Detected Magnetic Resonance and Near-Zero-Field Magnetoresistance

Stephen J. Moxim, *Member, IEEE*, James P. Ashton, *Member, IEEE*, Patrick M. Lenahan, *Fellow, IEEE*, Michael E. Flatté, *Member, IEEE*, Nicholas J. Harmon, and Sean W. King, *Member, IEEE*

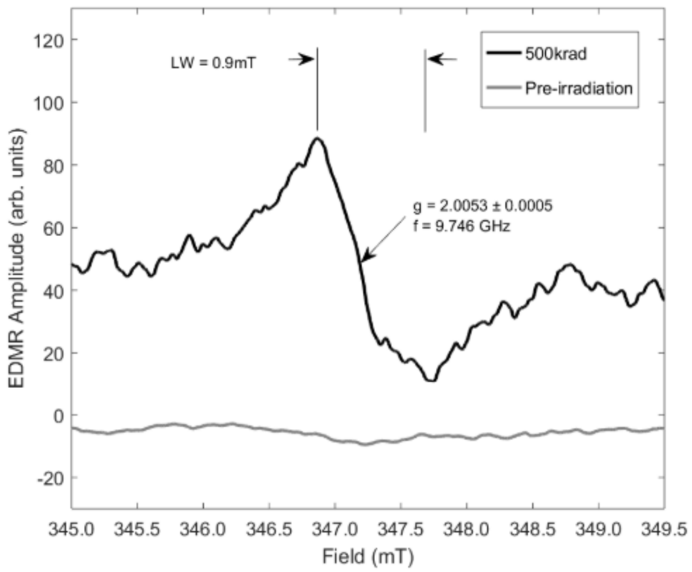

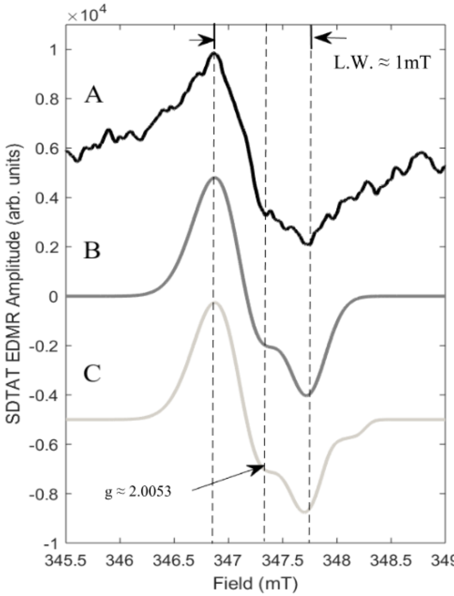

Fig. 9. Postirradiation, high-frequency SDTAT EDMR trace with magnetic field oriented perpendicular to the (100) plane (curve A). Derivative of simulated EPR trace with a 78% P_{b0} and 22% P_{b1} center contribution (curve *B*). Derivative of simulated EPR trace with a 77% P_{b0} and 21% P_{b1}, and 2% *E*' center contribution (curve C).

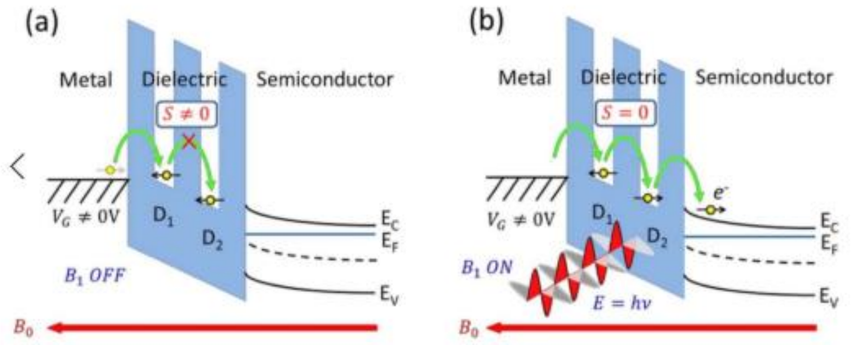

Fig. 1. Illustration of SDTAT. Tunneling is allowed from one defect to the other if spin angular momentum is conserved. Tunneling from one defect to the other is forbidden if angular momentum is not conserved. (a) However, if electromagnetic radiation satisfying the resonance condition is present, that radiation can "flip" paramagnetic defect spins, rendering previously forbidden tunneling events allowed (b), thereby increasing current across the dielectric.

How?

- Size and cont

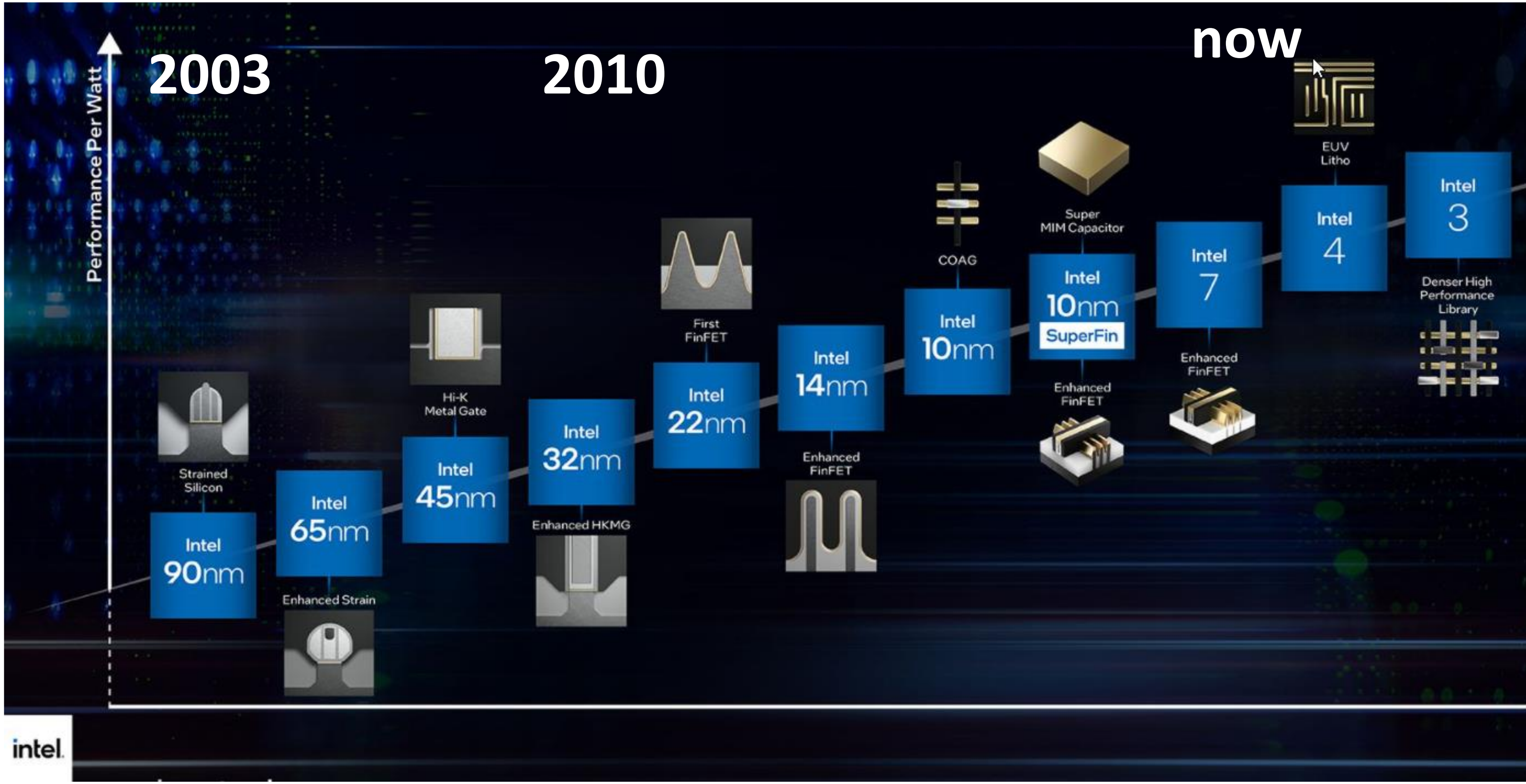

*technology node has become a marketing tool rather than a real physical feature description

Physical Basis For ESR (simplified)

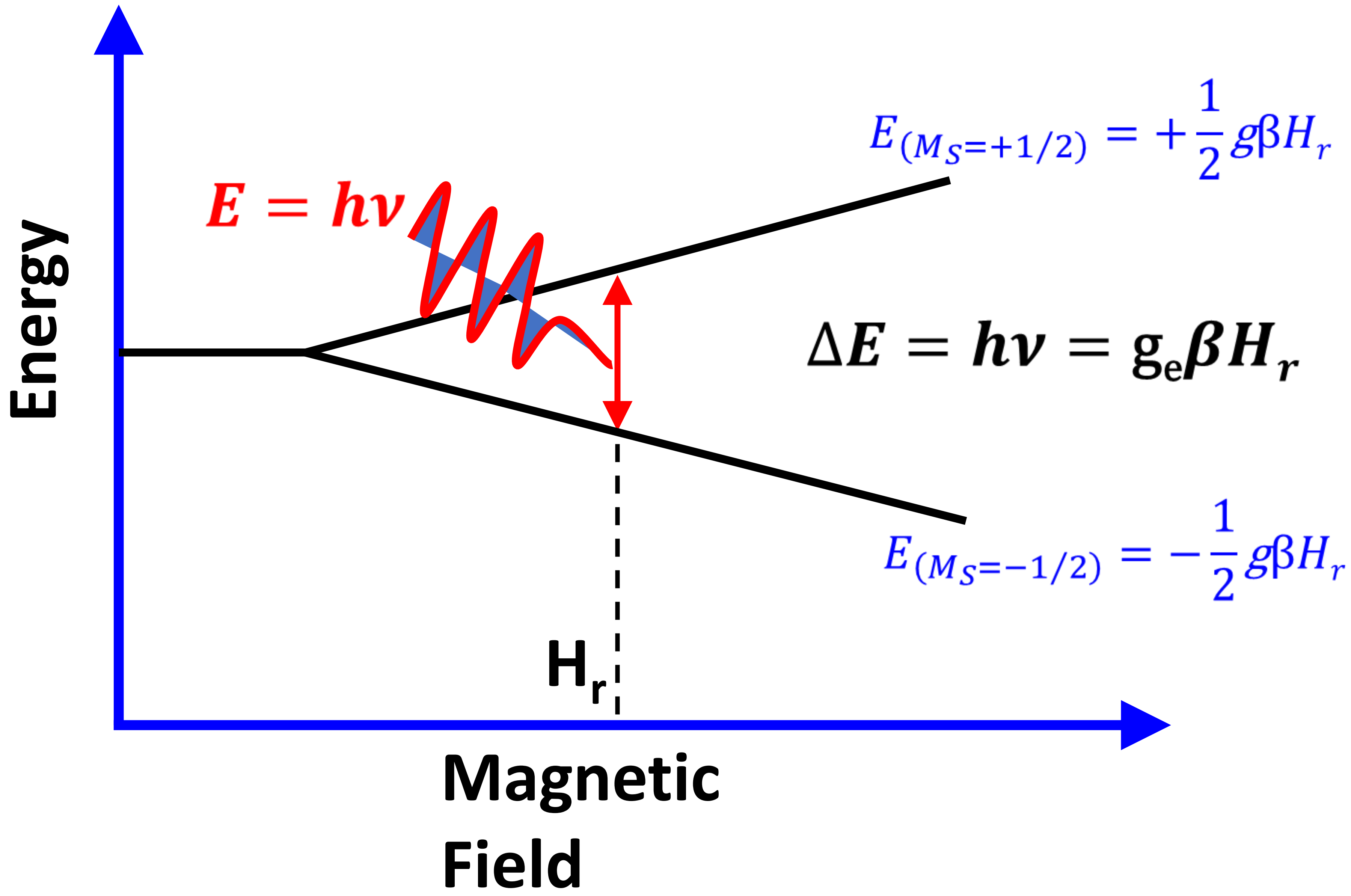

Physical Basis For ESR (simplified)